

Research Article

## ***Ziziphus rugosa* Leaves: Pharmacognostical Characters and Anti-Inflammatory Properties against Carrageenan-Induced Paw Edema**

Enugurthi Hari Krishna <sup>1</sup>

Kamatchi Sundara Saravanan <sup>1\*</sup>  

Judy Jays <sup>2</sup>   

<sup>1</sup> Department of Pharmacognosy, M. S. Ramaiah University of Applied Sciences, Bangalore, Karnataka, India

<sup>2</sup> Department of Pharmaceutical Chemistry, M. S. Ramaiah University of Applied Sciences, Bangalore, Karnataka, India

\*email: [sundarksharan@gmail.com](mailto:sundarksharan@gmail.com); phone: +919916530395

### **Keywords:**

Carrageenan  
Inflammation  
Leaves  
Pharmacognosy  
*Ziziphus rugosa*

### **Abstract**

*Ziziphus rugosa* belongs to the family Rhamnaceae, which includes many flowering species, primarily trees and shrubs, and sometimes vines. This study aims to describe the pharmacognostic characteristics and potential anti-inflammatory properties of *Z. rugosa* leaves. The pharmacognostical and preliminary phytochemical studies were performed following standard procedures. Acetone, ethanol, and aqueous extracts were screened for anti-inflammatory potential using the carrageenan-induced paw edema model. *Ziziphus rugosa* was identified by its evergreen nature, recurved hooks, and drupe-type fruits. Leaves are elliptic/rounded with cordate base exhibiting a dark green glossy upper surface and pubescent lower surface. They have a dorsiventral nature covering trichomes, collenchyma, sclerenchyma patch, and calcium oxalate crystals as a few key histological characters in the transverse section. In contrast, anamocytic stomata, covering trichomes, crystals, and fragments of vessels, are the imperative elements in powder. The extracts contain carbohydrates, alkaloids, glycosides, tannins, saponins, phenolic compounds, proteins, and flavonoids. The acetone extract at 400 and 200 mg/kg displays a maximum inflammation inhibition of 56.96% and 48.77% among the extracts, and the standard diclofenac sodium inhibits inflammation by 65.61% at 24 hours. The altered liver superoxide dismutase, glutathione, and malondialdehyde levels in the positive control group are significantly near normal in the treatment groups. The histopathological studies of treated animals show significant protection against paw and liver tissue damage. Pharmacognostical study outcomes aid in the identification of species along with ascertaining standardization parameters. Further fractionation of acetone extract followed by isolating compounds responsible for the anti-inflammatory activity would provide an alternative to managing inflammation.

Received: December 13<sup>th</sup>, 2023

1<sup>st</sup> Revised: January 25<sup>th</sup>, 2024

Accepted: February 3<sup>rd</sup>, 2024

Published: February 29<sup>th</sup>, 2024



© 2024 Enugurthi Hari Krishna, Kamatchi Sundara Saravanan, Judy Jays. Published by Institute for Research and Community Services Universitas Muhammadiyah Palangkaraya. This is an Open Access article under the CC-BY-SA License (<http://creativecommons.org/licenses/by-sa/4.0/>). DOI: <https://doi.org/10.33084/bjop.v7i1.6411>

## **INTRODUCTION**

Plants have been used from time immemorial for their therapeutic potential, with a belief that human well-being is dependent on natural sources<sup>1</sup>. This is evident from the wide usage of medicinal herbs in various folklore and indigenous systems of medicine across various regions. Thus, recognition of medicinal plants role in alleviating the disease conditions led to the search for plant-derived novel drugs from time to time<sup>2</sup>. The World Health Organization (WHO) report reinforces that around 80% of the population in developing countries satisfy their medical needs by relying on native systems of

medicine owing to the non-accessibility of modern systems of medicine, increased healthcare costs, cultural beliefs, safety, and efficacy concerns with novel and available marketed drugs<sup>3</sup>. A considerable percentage of the population in India still relies on Ayurveda, Siddha, and Unani systems for treating their various health ailments, and the possible reason for this could be the significant biodiversity accommodating around 45,000 plant species<sup>4</sup>. These plants contain diverse bioactive compounds with various pharmacological activities such as antiepileptic, anti-inflammatory, antidiabetic, anticancer, antioxidant, antimicrobial, antiulcer, analgesic, hepatoprotective, wound healing properties, and other<sup>5</sup>.

*Ziziphus rugosa* Lam. belongs to the family Rhamnaceae, which includes many flowering species, mostly trees and shrubs, and sometimes vines. Traditionally, various parts of this species, such as bark, flower, stem, fruit, and leaf, are used in conditions like diarrhea, menorrhagia, fever, mouth ulcer, cough, hypotension; treatment of wounds boils, rheumatism; as an aphrodisiac, astringent, and as a demulcent in treating broncho-pulmonary irritation<sup>6,7</sup>. Concurrently, the species is reported for its anti-inflammatory (root bark, root)<sup>8</sup>, antidiabetic (bark)<sup>9</sup>, antioxidant (stem)<sup>10</sup>, anthelmintic, antibacterial, insecticidal, antioxidant, cytotoxicity, CNS depressant and anxiolytic (fruit, pericarp, seed)<sup>11-14</sup> and analgesic, CNS depressant, antioxidant, hepatoprotective, cytotoxic and antimicrobial activities (leaf)<sup>15-17</sup>. Therefore, this study aims to determine the anti-inflammatory activity of *Z. rugosa* leaves extract along with preliminary pharmacognostic and phytochemical characteristics.

## MATERIALS AND METHODS

### Materials

Fresh, healthy *Z. rugosa* leaves were collected from Yelahanka, Bangalore, in December 2020. The collected leaves were washed with water and dried under shade. The plant material was authenticated by Dr. K. Ravikumar, Emeritus Professor, The University of Trans-Disciplinary Health Sciences and Technology (TDU), Foundation for Revitalization of Local Health Traditions (FRLHT), Bangalore, India. The herbarium was prepared per the standard curatorial practices<sup>18</sup> with collection voucher number FPH-PG-55 and submitted to the crude drug museum, PG Department of Pharmacognosy, along with a few leaf samples for future reference. Carrageenan and diclofenac sodium were obtained from Sigma Aldrich and Yarrow Chem Products, respectively. All other chemicals and reagents used in the present study were analytical grade.

### Methods

#### Pharmacognostical studies

The macroscopical characters were observed on intact *Z. rugosa* leaves and recorded. For microscopical studies, free-hand transverse sections of the midrib and petiole were obtained using a razor blade. The sections were stained with safranin, phloroglucinol, and concentrated HCl and observed for the histological characters. Powder microscopical characters were examined in coarse powder after clearing with chloral hydrate and stained with the aforementioned staining agents. Histochemical tests were performed to identify cell contents by treating the thin sections with phloroglucinol and concentrated HCl, Millon's reagent; Sudan III, iodine, ruthenium red, and ferric chloride solution<sup>19,20</sup>.

#### Physicochemical parameters

Loss on drying, yield to solvents (95% ethanol and water), and ash values (total, water-soluble, and acid-insoluble) were determined following standard procedures. About 1 g of the powder sample was separately treated with 50% H<sub>2</sub>SO<sub>4</sub>, 50% HNO<sub>3</sub>, 5% KOH, methanol, ethanol, acetone, 1 N HCl, 1 N methanolic NaOH, 1 N ethanolic NaOH, dilute ammonia solution, and visualized under 254, 365, and 425 nm for ultraviolet analysis. Successive solvent extraction was performed using solvents with varied polarity, such as *n*-hexane, chloroform, ethyl acetate, acetone, ethanol, and water. The obtained extracts were screened to identify the nature of contained phytochemicals<sup>21,22</sup>.

#### Experimental design

The acetone, ethanol, and aqueous extracts were selected for the evaluation of *in vivo* anti-inflammatory activity based on the preliminary phytochemical screening.

### FT-IR studies

The FT-IR spectra of *Z. rugosa* leaves extracts were recorded using Shimadzu FTIR-8400S based on diffuse reflectance spectroscopy. A background scan was run with potassium bromide and the extracts were mixed with potassium bromide in a ratio of 1 : 100 to obtain the spectra.

### Experimental animals

Seventy-two albino Wistar rats of 150–200 g was procured from the faculty animal house. The rats were allowed to acclimatize to the animal house environment for 14 days with feed and water ad libitum. The research protocol was approved by the Institutional Animal Ethics Committee of the Faculty with approval number XXIV/MSRFPH/COG/M-009, dated 27<sup>th</sup> November 2020, and conducted by the Committee for the Purpose of Control and Supervision of Experiments on Animals (CPCSEA) guidelines<sup>23</sup>.

### Acute toxicity study

The acute toxicity of the selected extracts was evaluated in Wistar rats following the Organization for Economic Co-operation and Development (OECD) 423 guidelines<sup>24</sup>. Animals were fasted overnight before dosing with water ad libitum. Six rats were administered 2000 mg/kg of each of the selected three extracts suspended in normal saline. Later, the animals were continuously monitored for 24 hours and subsequently for the next 14 days for any signs of abnormality or mortality.

### In vivo anti-inflammatory activity study

Carrageenan-induced paw edema model was used to evaluate the in vivo potential of the extracts. The animals were randomly divided into nine groups with each group containing six animals. The treatment details are summarized in **Table I**. Vehicle-treated and carrageenan control group rats received only the vehicle, while standard and extract treatment groups received respective treatments for seven days. On the 7<sup>th</sup> day, zero-hour paw volume was measured after the last dose of vehicle/extracts and standard administration.

Consequently, paw edema was induced in each rat by injecting 0.1 mL of 1% carrageenan in 1% normal saline into the sub-plantar tissues of the left hind paw. A further change in paw volume at 1, 2, 4, 6, 8, and 24 hours post-carrageenan administration was measured using a digital plethysmograph. Later, the animals were sacrificed by euthanasia to excise paw and liver tissues. The antioxidant parameters such as superoxide dismutase (SOD), glutathione (GSH), and malondialdehyde (MDA) levels were determined in liver samples, while histopathological studies were performed in both liver and paw tissues<sup>25-27</sup>.

**Table I.** Grouping and administration design.

Groups	Treatment
1	Vehicle control (normal saline)
2	Carrageenan control (0.1 mL, 1%)
3	Standard (Diclofenac sodium 10 mg/kg)
4	<i>Ziziphus rugosa</i> aqueous extract 200 mg/kg p.o.
5	<i>Ziziphus rugosa</i> aqueous extract 400 mg/kg p.o.
6	<i>Ziziphus rugosa</i> ethanol extract 200 mg/kg p.o.
7	<i>Ziziphus rugosa</i> ethanol extract 400 mg/kg p.o.
8	<i>Ziziphus rugosa</i> acetone extract 200 mg/kg p.o.
9	<i>Ziziphus rugosa</i> acetone extract 400 mg/kg p.o.

### Histopathological studies

Liver and paw tissues were washed with normal saline and stored in 10% formalin. The tissues were dehydrated and embedded in paraffin wax for sectioning. The sections were stained with hematoxylin and eosin for histopathological studies.

### Data analysis

The obtained results were statistically analyzed via one-way analysis of variance (ANOVA) and Tukey's Kramer multiple comparison tests using Graph-Pad InStat V-3 (<https://www.graphpad.com/scientific-software/instat/>). All the values were expressed as Mean  $\pm$  SEM (n = 6).



## RESULTS AND DISCUSSION

*Ziziphus rugosa* is a large evergreen straggling shrub/small tree of 3-6 m height with recurved hooks. The species is found distributed up to an altitude of 1800 m in dry deciduous forests. Flowers are in long-peduncled tomentose cymes, forming a panicle with globose buds and densely tomentose pedicels. Fruits are of drupe type, globose around 6-8 mm in diameter with one seed and white when ripe. Wood is moderately hard and red; while young branches were clothed with fulvous tomentum. The leaves are alternate, petiolate, elliptic/rounded with oblique or cordate base, and 5-7 cm long. The apex is rounded, retuse/mucronate, while the margin is serrulate. Fresh leaves are dark green, glossy on the upper surface, pale green to greyish-green, and pubescent on the lower side, while dry leaves are greyish-green. They possess three marked nerves almost traveling to the apex and are prominent on the lower surface. Petioles are tomentose and 6-12 mm in length. The taste of the leaf is mild, sweet, and with a characteristic odor (**Figure 1**).



**Figure 1.** Macroscopic characters of *Z. rugosa* (a: habit; b: leaf showing upper surface; c: leaf showing lower surface; d: flower; e: fruit; f: fresh leaf; g: dry leaf; h: twig showing recurved spine).

The transverse section of the leaf exhibited a dorsiventral nature with a prominent midrib on the lower side. The lamina comprises the upper epidermis, mesophyll, and lower epidermis. The upper epidermis comprises a single layer of small, tabular parenchyma cells covered with a cuticle. The mesophyll region is differentiated into single-layered upper palisade cells and spongy parenchyma. The lower epidermis comprises a single layer of small tabular parenchyma covering numerous trichomes. Vascular strands are found intermittently in the mesophyll regions of the lamina.

The upper epidermis is continuous in the midrib, while palisade cells are not continuous; instead, a patch of collenchyma appears in the midrib below the upper epidermis. The lower epidermis is continuous in the midrib region, with numerous unicellular covering trichomes. A patch of collenchyma is observed above the lower epidermis in the midrib region. "U" shaped vascular bundle is located in the midrib region with distinct phloem and xylem. The vascular bundle is surrounded by a patch of sclerenchyma cells. Spongy parenchyma cells are big, spherical, and located surrounding the sclerenchyma patch in the midrib. Druse and prismatic calcium oxalate crystals are found in collenchyma cells (**Figure 2**).

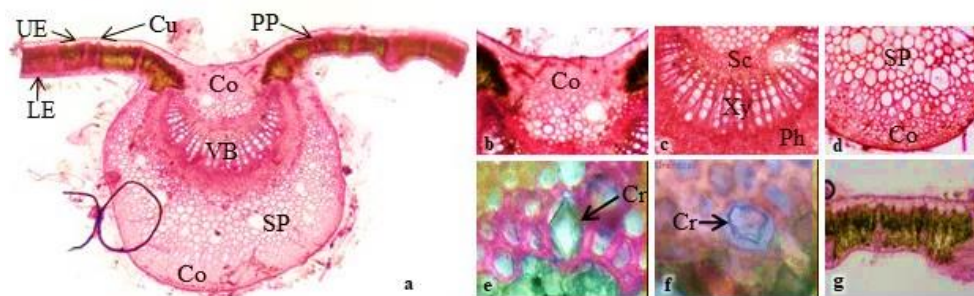


**Figure 2.** Microscopic characters of *Z. rugosa* leaf (a: transverse section showing midrib and lamina; b: midrib showing collenchyma below upper epidermis; c: midrib showing vascular bundle; d: midrib showing collenchyma and spongy parenchyma above lower epidermis; e,f: crystal; g: lamina (Co- collenchyma, Cr- crystal, Cu- cuticle, LE- lower epidermis, Ph- phloem, PP- palisade parenchyma, Sc- sclerenchyma, SP- spongy parenchyma, UE- upper epidermis, VB- vascular bundle, Xy- xylem).

The transverse section of the petiole shows an ovoid outline with a thin-walled single layer of epidermis covering trichomes. The cortex comprises 11-13 layers of thin-walled, loosely arranged compact parenchyma cells. One to two layers of thin-walled round to oval-shaped mucilage cells are found next to the cortex. Vascular bundles are collateral and rectangular, with a few layers of loosely arranged phloem cells. Loosely arranged spherical parenchyma, mucilage, and idioblast cells are observed at the center of the petiole (**Figure 3**). *Ziziphus rugosa* powder revealed the presence of parenchyma, covering trichomes, anomocytic stomata, fragments of vessels, and calcium oxalate crystals (**Figure 4**).

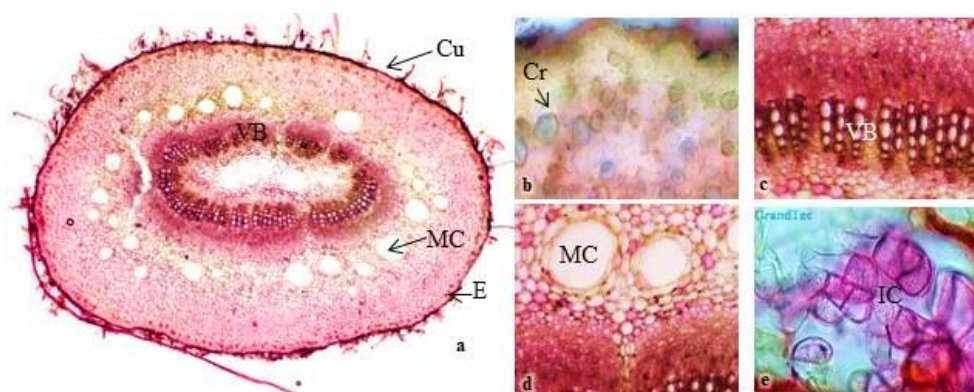


**Figure 3.** Microscopic characters of *Z. rugosa* petiole (a: transverse section showing epidermis, cortex, and vascular bundles; b: crystals in the cortical region; c: vascular bundle; d: mucilage cells; e: idioblast cells (Cr- crystal, Cu- cuticle, E- epidermis, VB- vascular bundle, MC- mucilage cell; IC- idioblast cell).

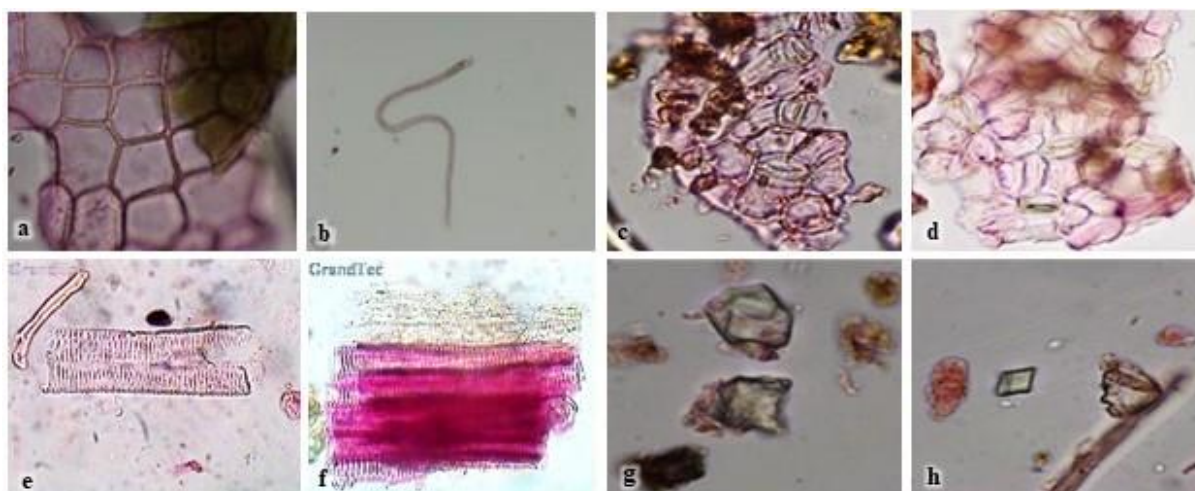


**Figure 4.** Powder characters of *Z. rugosa* leaf (a: parenchyma; b: covering trichome; c,d: stomata; e,f: fragments of vessels; g,h: crystals).



The contribution of plant-derived drugs in alleviating various diseased conditions is evident, and a resurgence in the usage of plant-based medicines has been observed in the recent past owing to efficacy and safety profile, accessibility, side effects of modern drugs, non-availability of a proper cure for specific disease conditions, microbial resistance, and other<sup>28,29</sup>. Acquiring maximum benefit from plant drugs depends on using the correct species claimed for particular indications. Hence, correctly identifying plant species by applying various scientific parameters is essential to garner the advantage of their possible and positive role in treating diseases. In this context, the first step towards identifying crude drugs is through macro- and microscopical characters<sup>30</sup> supported by herbarium specimen<sup>31</sup>. Macro and microscopical characters are essential as they provide insights into the diagnostic characters for identifying and differentiating plants belonging to diverse taxonomical hierarchies. *Ziziphus rugosa* can be identified by its evergreen nature with recurved hooks, long peduncled tomentose cymes, and drupe type of fruits, while leaves alternate with cordate base, pubescent, and with three prominent nerves on the lower side. Dorsiventral nature, covering trichomes, sclerenchymatous patch, druse, and prismatic calcium oxalate crystals are essential characteristics of its anatomical structure. Powder characters facilitate the establishment of the identity and quality of size-reduced plant materials. In this case, covering trichomes, stomata, crystals, and others, are the key characters to identify the leaf in powder form. Various physicochemical parameters determined will assist in ascertaining the Pharmacopoeial standards of the crude drug specimen<sup>32</sup>.

Histochemical tests revealed the presence of starch, proteins, lipids, tannins, mucilage, lignin, and cellulose, as positive reactions were noted with iodine solution (blue), Millon's reagent (red), Sudan III (red), FeCl<sub>3</sub> (bluish-black), ruthenium red solution (pink mucilage), and iodine with 60% sulfuric acid (yellowish brown), respectively. The various physicochemical parameters, such as loss on drying, yield to solvents, and ash values, were determined and represented in **Table II**. Then, leaf powder treated with various reagents exhibited characteristic colors under 254, 366, and 425 nm. The results are tabulated in **Table III**. The extraction results of *Z. rugosa* leaves powder are based on several parameters, including color, nature, and yield obtained with various solvents are as follows: *n*-hexane: dark green, sticky mass, 1.36%; chloroform: greenish brown, solid mass, 0.66%; ethyl acetate: greenish brown, solid mass, 2.84%; acetone: brownish green, sticky mass, 2.14%; 95% ethanol: greenish brown, sticky mass, 5.96%, and water: brown, solid, 7.66%. The extracts possess various phytoconstituents such as alkaloids, carbohydrates, glycosides, proteins, phenolics, tannins, saponins, and flavonoids. The phytochemical study outlines the quantity and nature of phytoconstituents present in the sample, which can be further utilized to establish biomarker compounds that aid in proper identification and help to determine the purity of plant drug materials<sup>33</sup>. In addition to powder characters, fluorescence studies afford some diagnostic information on the identification and verification of the quality of the sample based on fluorescence exhibited under diverse wavelengths when treated with different reagents and solvents<sup>34</sup>.

The spectra of various extracts of *Z. rugosa* leaves are illustrated in **Figure 5**. The FT-IR spectra signified the presence of diverse functional groups, and variations in peaks among all the extracts were also observed<sup>35</sup>. Some of the essential functional groups visualized were 1°, 2° amines (NH stretching, 3550-3230 cm<sup>-1</sup>), amides (C=O stretching, 1652 cm<sup>-1</sup>) aldehyde (CH stretching, 2900-2800 cm<sup>-1</sup>) in *n*-hexane extract; aromatic CH (CH stretching, 1629-1427 cm<sup>-1</sup>), 1° amines (NH stretching, 3294-3423 cm<sup>-1</sup>), phenol (OH stretching, 3569-3529 cm<sup>-1</sup>) in chloroform extract; aromatic (CH stretching out of plane bend, 966 cm<sup>-1</sup>), amines (C-N stretching, 1764-1076 cm<sup>-1</sup>), 1° amines (C=N stretching, 2252 cm<sup>-1</sup>), amines (NH stretching, 3452-3404 cm<sup>-1</sup>), alkanes (CH stretching, 2921 cm<sup>-1</sup>) in ethyl acetate extract; alkane (CH stretching, 2927-2852 cm<sup>-1</sup>), alkene (CH stretching, 2476-2619 cm<sup>-1</sup>), ketone (C=O stretching, 1716-1458 cm<sup>-1</sup>), aromatic alkene (C-C stretching, 1515-1458 cm<sup>-1</sup>) in acetone extract; alcohol (OH stretching, 3851-3919 cm<sup>-1</sup>), nitrile (C≡N stretching, 2354-2210 cm<sup>-1</sup>), aldehyde (CHO stretching, 1955-1863 cm<sup>-1</sup>), amines (C-N stretching, 1207-1035 cm<sup>-1</sup>) in ethanol extract; and 1°, 2° amines (NH stretching, 3500-3100 cm<sup>-1</sup>), alkyl (CH<sub>3</sub> bending, 1153 cm<sup>-1</sup>) in the aqueous extract. The FT-IR spectra are considered a reliable option to detect the bio-molecular composition and provide valuable information on the various classes of compounds present in the extracts<sup>36</sup>.

**Table II.** Physicochemical parameters of *Z. rugosa* leaves.

Loss on drying (%)	Ash value (%)			Yield to solvent (%)	
	Total ash	Water-soluble	Acid-insoluble	Water	95% ethanol
8.66	5.55	1.11	0.66	13.86	5.60

**Table III.** Fluorescence analysis of *Z. rugosa* leaves.

Reagents	Visible light	UV light	
		Short wave (254 nm)	Long wave (365 nm)
Powder as such	Sultry	Sultry	Mehandi N
50% H <sub>2</sub> SO <sub>4</sub>	Vivid green	Mehandi N	Dark drama
50% HNO <sub>3</sub>	Copper leaf	Copper	Vivid green
5% KOH	Green gold	Meadow path	Mehandi N
Methanol	Mehandi N	Vivid green	Pine N
Ethanol	Mehandi N	Green gold	Pine N
Acetone	Dark drama	Amazon moss	Meadow path
1 N HCL	Sultry	Mehandi N	Green gold
1 N methanolic NaOH	Green gold	Dark drama	Vivid green
1 N ethanolic NaOH	Mehandi N	Mehandi N	Dark drama
Diluted NH <sub>3</sub> solution	Green gold	Meadow path	Amazon moss

Note: All color comparison is based on the “Asian paints” premium gloss enamel card, Asian Paints Limited, Mumbai

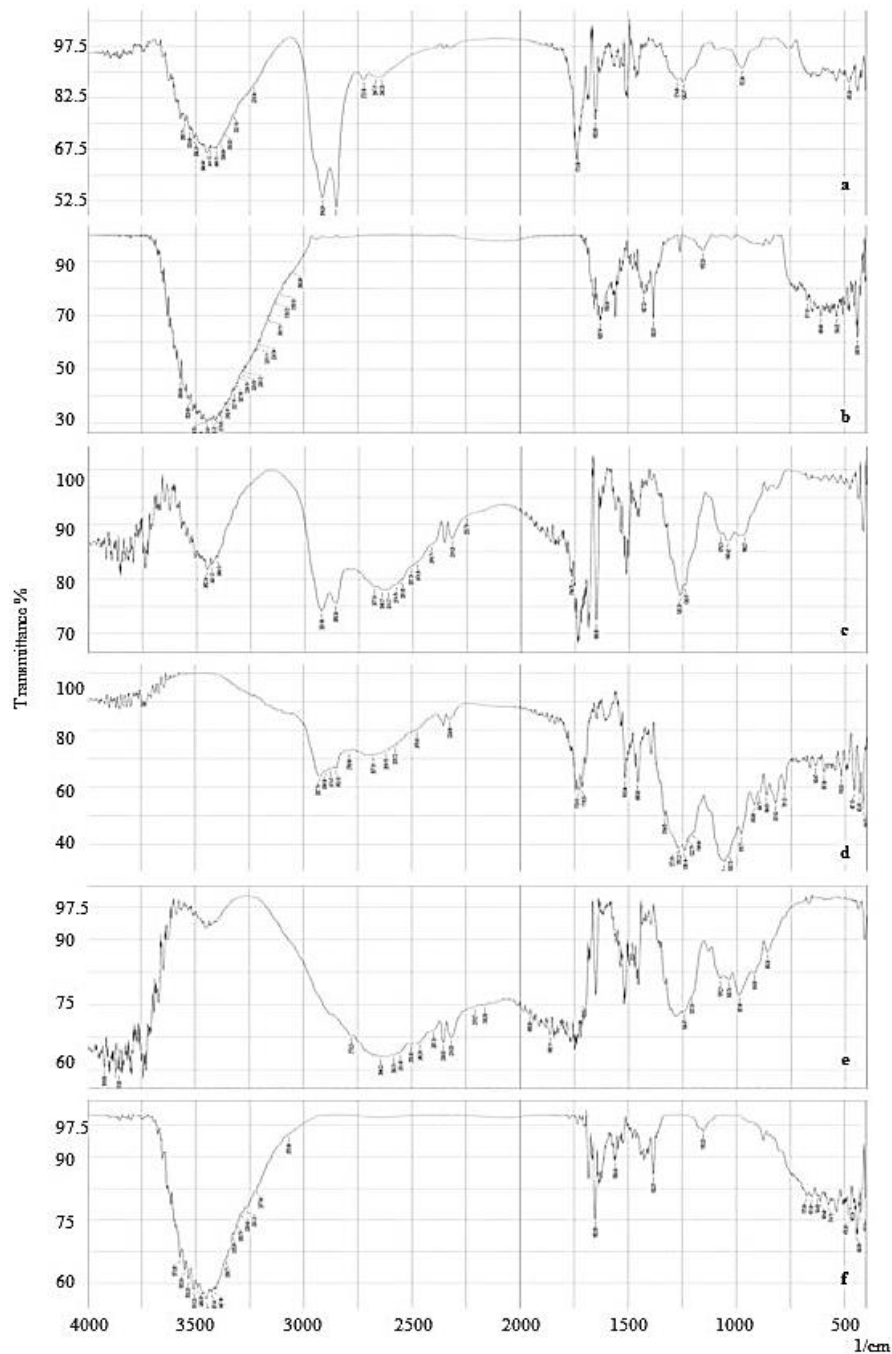


**Figure 5.** FT-IR spectra of various *Z. rugosa* leaves extracts (a: *n*-hexane extract; b: chloroform extract; c: ethyl acetate extract; d: acetone extract; e: ethanol extract; f: aqueous extract).

Acute toxicity studies of acetone, ethanol, and aqueous extracts of *Z. rugosa* leaves were performed following OECD 423 guidelines. None of the extracts exhibited any signs of abnormality or mortality at 2000 mg/kg dose either during short-term (24 hours) or long-term observation (14 days). Hence,  $\frac{1}{5}$ <sup>th</sup> (400 mg) and  $\frac{1}{10}$ <sup>th</sup> (200 mg) of the tolerated dose were used for *in vivo* evaluation<sup>19</sup>. An acute toxicity study is essential to understand the toxicological profile of the substance being administered to animals either as a single dose or over short-term exposure<sup>37</sup>. Administration of aqueous, acetone, and ethanol extract at 2000 mg/kg to animals did not exhibit any toxic symptoms or mortality over a 24-hour observation period. Hence 200 mg/kg and 400 mg/kg of these extracts were finalized for further *in vivo* anti-inflammatory activity study. Carrageenan injection significantly developed the edema and a maximum increase in paw volume was noticed at four hours ( $23.98 \pm 0.32\%$ ). The percentage increase in paw volume at 24 hours in carrageenan control animals was  $8.55 \pm 0.42\%$ , while the diclofenac sodium treated animals exhibited a significant decrease in percentage increase of paw volume ( $2.94 \pm 0.20\%$ ) representing the anti-inflammatory effect. The percentage increase in paw volume of the *Z. rugosa* leaves extract administered animals at 24 hours was as follows: aqueous extract (200 mg/kg:  $6.82 \pm 0.47\%$ ; 400 mg/kg:  $5.28 \pm 0.42\%$ ), ethanol extract (200 mg/kg:  $5.62 \pm 0.54\%$ ; 400 mg/kg:  $5.25 \pm 0.60\%$ ) and acetone extract (200 mg/kg:  $4.38 \pm 0.30\%$ ; 400 mg/kg:  $3.68 \pm 0.22\%$ ), as shown in Figure 6.

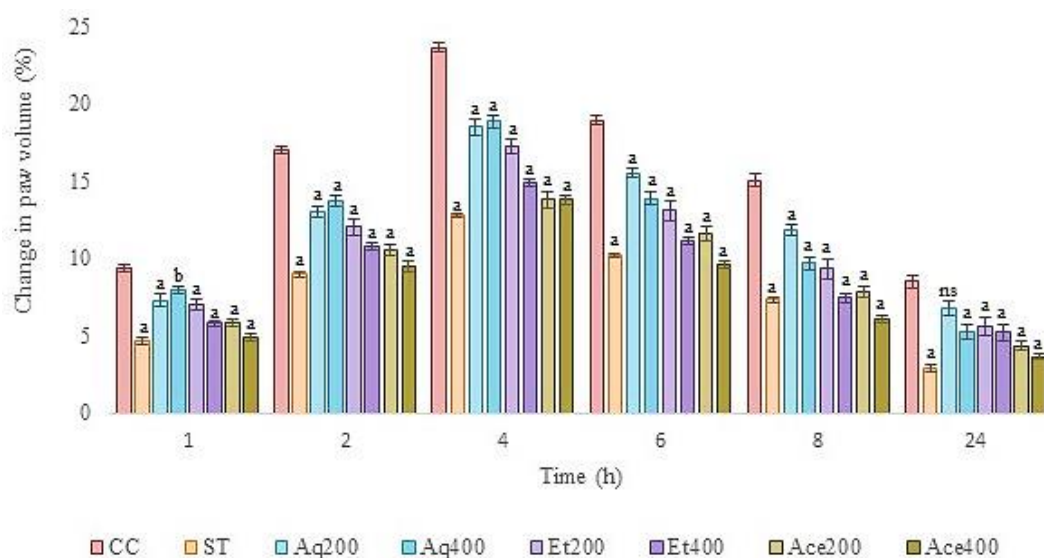


**Figure 6.** Change of paw volumes in carrageenan-induced paw edema at 1, 2, 4, 6, 8, and 24 hours (CC- carrageenan control; ST- standard treated; Aq200- aqueous extract 200 mg/kg; Aq400- aqueous extract 400 mg/kg; Et200- ethanol extract 200 mg/kg; Et400- ethanol extract 400 mg/kg; Ace200- acetone extract 200 mg/kg; Ace400- acetone extract 400 mg/kg). Values expressed as mean  $\pm$  SEM (n = 6). ap <0.001, bp <0.05. standard and extract-treated group Vs. carrageenan control group.

Diclofenac sodium at 10 mg/kg inhibited the inflammation by 65.61% at 24 hours. Maximum percentage inhibition of inflammation was observed with acetone extract, 56.96% at 400 mg/kg and 48.77% at 200 mg/kg at 24 hours among the extract-treated groups. The percentage inhibition of inflammation noticed with ethanol extract was 38.6% (400 mg/kg) and 34.27% (200 mg/kg), while aqueous extract exhibited 38.25% and 20.23% of inflammation inhibition at the low and high doses, respectively.

Decreased liver GSH levels were observed in animals of the carrageenan control group compared to vehicle-treated animals, indicating an alteration in antioxidant status<sup>38</sup>. Administration of test substances (aqueous, ethanol, and acetone extracts) significantly increased the GSH levels. On the other hand, carrageenan control group animals exhibited an increase in liver MDA levels compared to vehicle-treated rats, and these elevated MDA levels were significantly decreased in various extract-treated animals at both doses. Liver SOD levels of carrageenan control animals were decreased as compared to control rats, and the trend was similar to that of liver GSH levels<sup>39</sup>. None of the extracts at low doses demonstrated a substantial increase in SOD. Yet, the animals administered with high doses (400 mg/kg) of all the extracts revealed a significant increase in SOD levels (Figure 7).



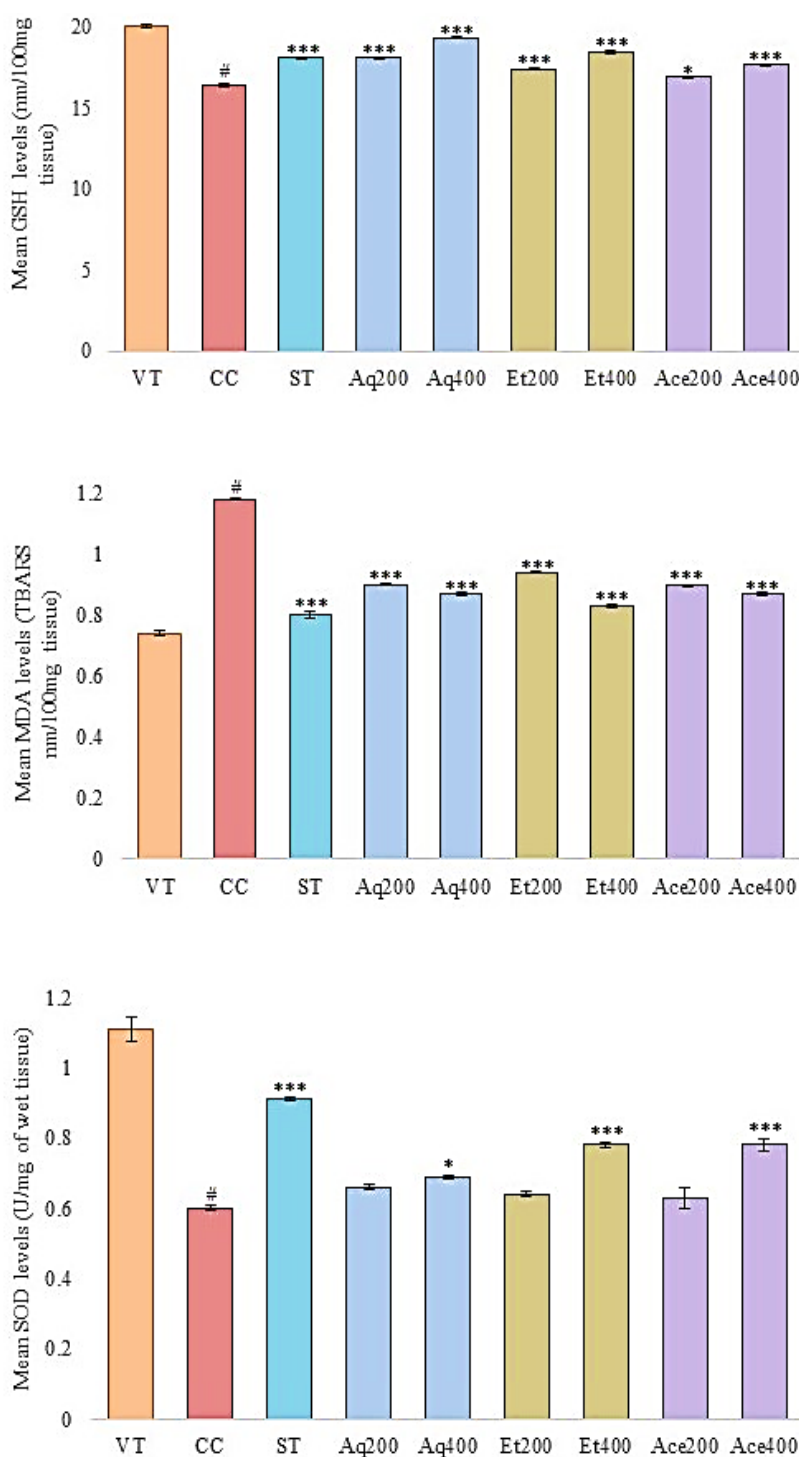


**Figure 7.** Mean liver GSH, MDA, and SOD levels (VT- vehicle-treated; CC- carrageenan control; ST- standard treated; Aq200- aqueous extract 200 mg/kg; Aq400- aqueous extract 400 mg/kg; Et200- ethanol extract 200 mg/kg; Et400- ethanol extract 400 mg/kg; Ace200- acetone extract 200 mg/kg; Ace400- acetone extract 400 mg/kg. Values expressed as mean  $\pm$  SEM. (n=6). \*\*\*p < 0.001; \*p < 0.05- standard and extract treated group Vs. carrageenan control group; #p < 0.001- carrageenan control group Vs. vehicle-treated group).

Liver histopathological photomicrographs of animals about various groups are represented in [Figure 8](#). Vehicle-treated group liver specimen confirms steady lobular architecture with usual hepatic cells and well-maintained cytoplasm exhibiting fine sinusoidal lines. The perivenular area was accompanied by a nucleus with complete architecture. Normal central veins, Kupffer cells, and endothelial cells with no structural alterations are visible. Histology of carrageenan control group livers exhibited degenerative sequence, blood-filled sinusoids, and nuclei with varied sizes and shapes. Cloudy swelling and large or focal necrosis of hepatocytes with granulated cytoplasm were detected, along with some fatty changes.

The nuclei of some cells were pyknotic or karyorrhectic, while megalocytosis with marginal hyperchromasia was also observed. Standard drug-treated group liver illustrated intact architecture with few neutrophil infiltrations and mild hepatocyte degeneration. Bi-nucleated hepatocytes with cystic lesions and perivascular inflammation were noticed. Vacuolization in the cytoplasm and focal nucleomegaly were also observed. Animals administered with 200 mg/kg aqueous extract demonstrated epithelial hyperplasia and increased connective tissues in portal gaps. Hepatocytes revealed vacuolar degeneration and signs of necrosis. Concomitantly, intrahepatic cholestasis, absence of lesions in the interface portal space with normal hepatocytes, and an increase in the number of perisinusoidal cells were noticed in the liver histopathology of animals treated with 400 mg/kg aqueous extract. The hepatic structure of rats administered with 200 mg/kg of ethanol extract illustrated hemorrhage between sinusoids and fibrocystic lesions with inflammatory cells. No structural loss was observed with periportal inflammatory cells. Ethanol extract 400 mg/kg treated group animal liver specimen demonstrated dilated sinuses filled with erythrocytes and congested blood vessels. Cystic lesions, focal areas of nuclear enlargement, and pyknosis were observed. Very large bi-nucleated hepatocytes with prominent nucleolus revealed mild hepatic damage. Animals of the group that received a low dose of acetone extract (200 mg/kg) displayed an intact architecture but with inflammatory infiltration, while the high dose (400 mg/kg) treated group revealed mild vacuolar degeneration and fibrosis transition.

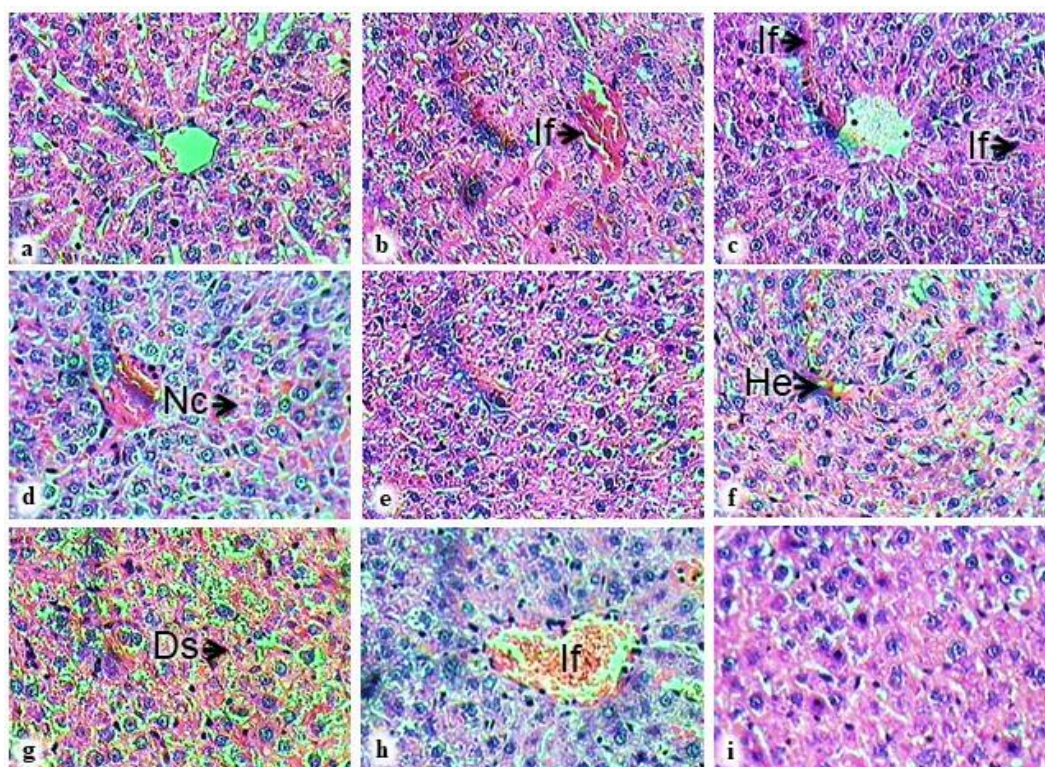


**Figure 8.** Representative photomicrographs of liver sections (a: vehicle control, 10x; b: carrageenan control, 10x; c: standard treated 10x; d: aqueous extract 200 mg/kg, 10x; e: aqueous extract 400 mg/kg, 10x; f: ethanol extract 200 mg/kg, 10x; g: ethanol extract 400 mg/kg, 10x; h: acetone extract 200 mg/kg, 10x; i: acetone extract 400 mg/kg, 10x. If: infiltration; Nc: necrosis; He: hemorrhage; Ds: dilated sinuses).

Paw tissue specimens from different groups were observed for histopathological severity of inflammatory response based on tissue alterations (**Figure 9**). Examined sections from vehicle control animals showed a typical arrangement of the epidermis, dermis with numerous sebaceous glands, and sub-epidermal and subcutaneous layers. Meanwhile, infiltrations with polymorphonuclear inflammatory cells, injured blood vessels, detachment of epidermal layer, and severe dermal inflammatory reaction were observed in paw tissue of carrageenan control animals. Rats treated with standard drugs demonstrated a conspicuous regeneration with vasculitis and hyperemia around the vessels in the dermis, besides mild epithelial hyperplasia and sub-epidermal edema. Aqueous extract 200 mg/kg treated group animals exhibited marked cellular diffused infiltration in the connective tissues. Acute edematosis in the epidermis as well as in the dermis and moderate dermal inflammatory reaction were also apparent. A reduction in inflammatory cells with evident morphological



regeneration of the dermis and epidermis is noticed in the group administered with 400 mg/kg of aqueous extract. Treatment with 200 mg/kg of ethanol extract presented a near-normal structure with less inflammation alongside distended blood vessels with inflammatory cells and vast numbers of adipocytes. In contrast, a visible reduction in the number of inflammatory cells within the dermis and an importunate regeneration of epidermal layers were evident in the tissue biopsy of rats treated with a high dose of ethanol extract (400 mg/kg). Mild epithelial hyperplasia and inflammatory reaction-related inter-muscular infiltration with many neutrophils were detected in the histopathology of 200 mg/kg of acetone extract treated rats. In contrast, an influx of inflammatory cell infiltration, considerable numbers of inflammatory cells, and subepidermal edema, accompanied by regenerative changes within the epidermis, were observed in 400 mg/kg acetone extract-treated animals.

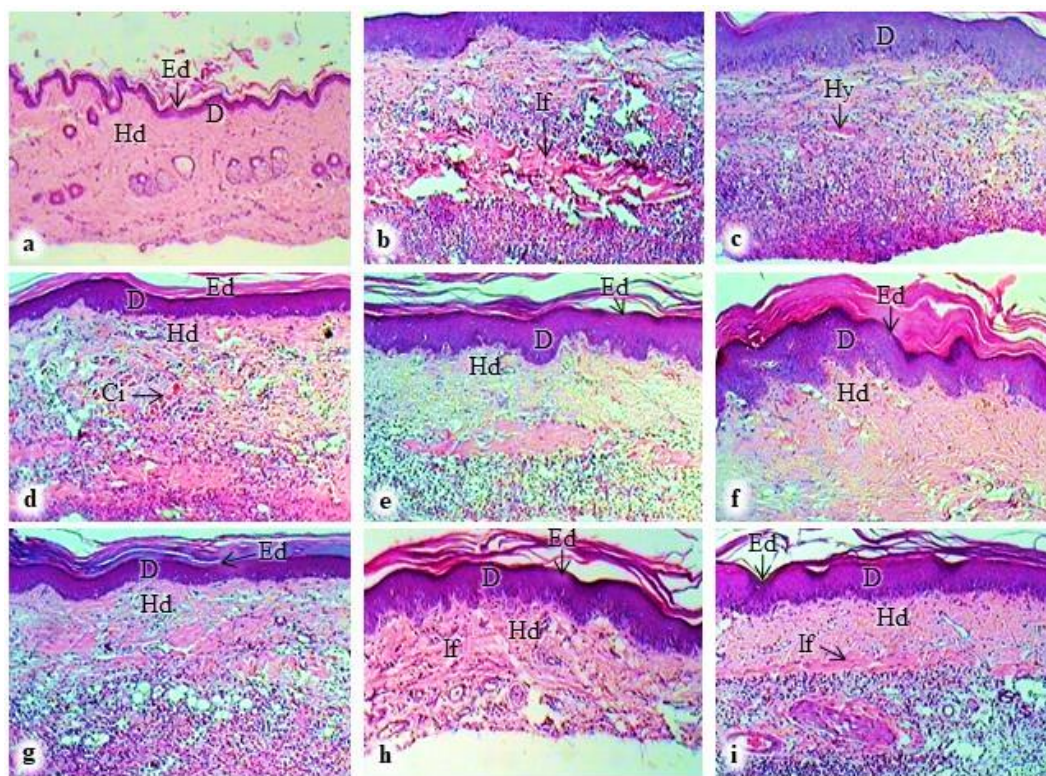


**Figure 9.** Representative photomicrographs of paw tissue sections (a: Vehicle control, 4x; b: carrageenan control, 10x; c: standard treated, 10x; d: aqueous extract 200 mg/kg, 10x; e: aqueous extract 400 mg/kg, 10x; f: ethanol extract 200 mg/kg, 10x; g: ethanol extract 400 mg/kg, 10x; h: acetone extract 200 mg/kg, 10x; i: acetone extract 400 mg/kg, 10x. Ed: epidermis; D: dermis; Hd: hypodermis; If: infiltration; Ci: cellular infiltration).

Paw edema was induced using carrageenan in animals administered with aqueous, acetone, and ethanol extract doses for seven days. The inflammation caused can be attributed to the release of histamine, serotonin, and kinin at the initial phase, followed by prostaglandin-like substances in the later stage<sup>40</sup>. Results indicated that acetone extract offered better protection than aqueous and ethanol extract. The protection offered may be ascribed to the diverse class of phytochemicals in the extract and might have been influenced by the probable antioxidant property. Free radicals are ascribed to play a role in carrageenan-induced inflammation<sup>41</sup>. Malondialdehyde (MDA), a metabolic product of lipid peroxidation, rises due to oxidative stress, and administration of acetone extract lowers the carrageenan-induced elevation of MDA levels, which is suggestive of the antioxidant property of the extract. The antioxidant effect was also witnessed in the liver histopathological study with mild vacuolar degeneration and fibrosis transition in the acetone extract-treated animals against the blood-filled sinusoids, cloudy swellings, and focal necrosis in the carrageenan control group. On the other hand, paw tissue histopathological study of the carrageenan control group revealed polymorphonuclear inflammatory cells, injured blood vessels, and severe dermal inflammatory reaction, while acetone extract treated groups exhibited only a considerable number of inflammatory cells<sup>42</sup>.



## CONCLUSION

The study provides insight into various pharmacognostical parameters to identify and authenticate *Z. rugosa* leaves. Phytochemical screening can be further explored to establish chemical marker compounds. Additionally, well-established pharmacognostic and phytochemical characteristics might lead to laying down Pharmacopoeial standards for the crude drug. The acetone extract may further be fractionated to determine the active fraction, followed by the isolation of active constituents responsible for the anti-inflammatory potential.

## ACKNOWLEDGMENT

The authors are thankful to the late Dr. Mohammad Azamthulla, Assistant Professor, Department of Pharmacology, Faculty of Pharmacy, M. S. Ramaiah University of Applied Sciences, whom the authors remember with utmost respect for his guidance and assistance in carrying out the study. The authors are also thankful to Dr. J. Anbu, Professor and Head, and Ms. Gouri Nair, Assistant Professor, Department of Pharmacology, Faculty of Pharmacy, M. S. Ramaiah University of Applied Sciences, for their support in this study.

## AUTHORS' CONTRIBUTION

**Conceptualization:** Enugurthi Hari Krishna, Kamatchi Sundara Saravanan

**Data curation:** Enugurthi Hari Krishna

**Formal analysis:** Enugurthi Hari Krishna, Kamatchi Sundara Saravanan

**Funding acquisition:** -

**Investigation:** Enugurthi Hari Krishna

**Methodology:** Kamatchi Sundara Saravanan, Judy Jays

**Project administration:** Kamatchi Sundara Saravanan, Judy Jays

**Resources:** Kamatchi Sundara Saravanan, Judy Jays

**Software:** -

**Supervision:** Kamatchi Sundara Saravanan, Judy Jays

**Validation:** Kamatchi Sundara Saravanan, Judy Jays

**Visualization:** Enugurthi Hari Krishna, Kamatchi Sundara Saravanan, Judy Jays

**Writing - original draft:** Enugurthi Hari Krishna

**Writing - review & editing:** Kamatchi Sundara Saravanan, Judy Jays

## DATA AVAILABILITY

None.

## CONFLICT OF INTEREST

The authors declare there is no conflict of interest.

## REFERENCES

1. Abdallah EM, Alhatlani BY, Menezes RdP, Martins CHG. Back to Nature: Medicinal Plants as Promising Sources for Antibacterial Drugs in the Post-Antibiotic Era. *Plants*. 2023;12(17):3077. DOI: [10.3390/plants12173077](https://doi.org/10.3390/plants12173077); PMCID: [PMCID: 37687324](https://pubmed.ncbi.nlm.nih.gov/37687324/); PMID: 37687324

2. Eshete MA, Molla EL. Cultural significance of medicinal plants in healing human ailments among Guji semi-pastoralist people, Suro Barguda District, Ethiopia. J Ethnobiol Ethnomed. 2021;17(1):61. DOI: [10.1186/s13002-021-00487-4](https://doi.org/10.1186/s13002-021-00487-4); PMCID: [PMC8524801](https://pubmed.ncbi.nlm.nih.gov/PMC8524801/); PMID: [34663365](https://pubmed.ncbi.nlm.nih.gov/34663365/)
3. Ampomah IG, Malau-Aduli BS, Seidu AA, Malau-Aduli AEO, Emeto TI. Perceptions and Experiences of Orthodox Health Practitioners and Hospital Administrators towards Integrating Traditional Medicine into the Ghanaian Health System. Int J Environ Res Public Health. 2021;18(21):11200. DOI: [10.3390/ijerph182111200](https://doi.org/10.3390/ijerph182111200); PMCID: [PMC8582872](https://pubmed.ncbi.nlm.nih.gov/PMC8582872/); PMID: [34769719](https://pubmed.ncbi.nlm.nih.gov/34769719/)
4. Krupa J, Sureshkumar J, Silambarasan R, Priyadarshini K, Ayyanar M. Integration of traditional herbal medicines among the indigenous communities in Thiruvavur District of Tamil Nadu, India. J Ayurveda Integr Med. 2019;10(1):32-7. DOI: [10.1016/j.jaim.2017.07.013](https://doi.org/10.1016/j.jaim.2017.07.013); PMCID: [PMC6470307](https://pubmed.ncbi.nlm.nih.gov/PMC6470307/); PMID: [30120054](https://pubmed.ncbi.nlm.nih.gov/30120054/)
5. Ullah A, Munir S, Badshah SL, Khan N, Ghani L, Poulson BG, et al. Important Flavonoids and Their Role as a Therapeutic Agent. Molecules. 2020;25(22):5243. DOI: [10.3390/molecules25225243](https://doi.org/10.3390/molecules25225243); PMCID: [PMC7697716](https://pubmed.ncbi.nlm.nih.gov/PMC7697716/); PMID: [33187049](https://pubmed.ncbi.nlm.nih.gov/33187049/)
6. DeFilipps RA, Krupnick GA. The medicinal plants of Myanmar. PhytoKeys. 2018;102:1-341. DOI: [10.3897/phytokeys.102.24380](https://doi.org/10.3897/phytokeys.102.24380); PMCID: [PMC6033956](https://pubmed.ncbi.nlm.nih.gov/PMC6033956/); PMID: [30002597](https://pubmed.ncbi.nlm.nih.gov/30002597/)
7. Manjunatha E, Vedigounder M, Geetha KM, Nandeesh R, Palaksha MN. Review on A Wild Medicinal Plant: Ziziphus rugosa. Int J Pharm Sci Rev Res. 2020;62(2):40-4.
8. Yadav A, Singh P. Analgesic and anti-inflammatory activities of Zizyphus rugosa root barks. J Chem Pharm Res. 2010;2(3):255-9.
9. Mohamad S, Frank RP, Shameem AAK, John NT, Malieka RB. In vivo and in vitro antidiabetic activity of Ziziphus rugosa Lam. Bark. Int J Univers Pharm Bio Sci. 2013;2(5):457-68.
10. Hossain MS, Uddin N, Islam AFMM, Hasan AHMN, Hossain MM, Hasan MR, et al. Evaluation of in vitro antioxidant and brine shrimp lethality activities of different stem extracts of Zizyphus rugosa Lam. J Food Meas Charact. 2015;9(3):454-62. DOI: [10.1007/s11694-015-9253-4](https://doi.org/10.1007/s11694-015-9253-4)
11. Sarala P, Krishnamurthy SR. Phytochemical screening and anthelmintic activity of Zizyphus rugosa Lamk. Int J Pharm Sci Rev Res. 2019;57(1):13-20.
12. Prashith KTR, Raghavendra HL, Vinayaka KS. Evaluation of pericarp and seed extract of Zizyphus rugosa Lam. for cytotoxic activity. Int J Pharm Biol Arch. 2011;2(3):887-90.
13. Prashith KTR, Vinayaka KS, Mallikarjun N, Bharath AC, Shailendra KB, Rakesh KMC, et al. Antibacterial, Insecticidal and Free radical scavenging activity of methanol extract of Zizyphus rugosa Lam. (Rhamnaceae) fruit pericarp. Pharmacogn J. 2011;2(18):65-9. DOI: [10.1016/S0975-3575\(11\)80028-3](https://doi.org/10.1016/S0975-3575(11)80028-3)
14. Gawande RK, Tare HL, Shende VS, Bongirwar AA, Deore SR, Dama GY. Anxiolytic and CNS depressant activity of extracts obtained from seeds of Zizyphus rugosa. Int J Curr Pharm Clin Res. 2011;1(1):21-32.
15. Bulbul IJ, Khan MF, Rashid MA. Analgesic and central nervous system depressant activities of methanol extract of Zizyphus rugosa Lam. leaves. Afr J Pharm Pharmacol. 2016;10(40):849-53. DOI: [10.5897/AJPP2015.4423](https://doi.org/10.5897/AJPP2015.4423)
16. Parashar S, Uplanchiwar V, Gautam RK, Goyal S. In vitro antioxidant and in vivo hepatoprotective activity of ethanolic extract of Zizyphus rugosa Lam. Leaves. Indian Drugs. 2019;56(7):69-75. DOI: [10.53879/id.56.07.11577](https://doi.org/10.53879/id.56.07.11577)
17. Hossain MS, Uddin N, Hasan N, Hossain MP, Mondal M, Islam T, et al. Phytochemical, cytotoxic, in-vitro antioxidant and anti-microbial investigation of ethanolic leaf extract of Zizyphus rugosa Lam. IOSR J Pharm Biol Sci. 2013;6(5):74-81. DOI: [10.9790/3008-0657481](https://doi.org/10.9790/3008-0657481)

18. Jain SK, Rao RR. A Hand Book of Field and Herbarium Methods. New Delhi: Today and Tomorrow's Printers and Publishers; 1976. p. 22–61.
19. Kumar SM, Azamthulla M, Saravanan KS. Pharmacognostical evaluation and anti-convulsant property of *Annona reticulata* Linn. (Annonaceae) root. *Futur J Pharm Sci.* 2021;7:173. DOI: [10.1186/s43094-021-00319-y](https://doi.org/10.1186/s43094-021-00319-y)
20. Singh A, Saharan VA, Bhandari A. Pharmacognostic standardization with various plant parts of *Desmostachya bipinnata*. *Pharm Biol.* 2014;52(3):298–307. DOI: [10.3109/13880209.2013.834367](https://doi.org/10.3109/13880209.2013.834367); PMID: [24107271](https://pubmed.ncbi.nlm.nih.gov/24107271/)
21. Kumar V, Sharma AK, Rajput SK, Pal M, Dhiman N. Pharmacognostic and pharmacological evaluation of *Eulaliopsis binata* plant extracts by measuring in vitro/ in vivo safety profile and anti-microbial potential. *Toxicol Res.* 2018;7(3):454–64. DOI: [10.1039/c8tx00017d](https://doi.org/10.1039/c8tx00017d); PMCID: [PMC6062097](https://pubmed.ncbi.nlm.nih.gov/pmc/PMC6062097/); PMID: [30090595](https://pubmed.ncbi.nlm.nih.gov/30090595/)
22. Kokate CK, Purohit AP, Gokhale SB. Pharmacognosy. In: *Terpenoids*. 21<sup>st</sup> Edition. Pune: Nirali Prakashan; 2017. p. 377–8.
23. Saraf SK, Kumaraswamy V. Basic research: Issues with animal experimentations. *Indian J Orthop.* 2013;47(1):6–9. DOI: [10.4103/0019-5413.106882](https://doi.org/10.4103/0019-5413.106882); PMCID: [PMC3601236](https://pubmed.ncbi.nlm.nih.gov/pmc/PMC3601236/); PMID: [23532705](https://pubmed.ncbi.nlm.nih.gov/23532705/)
24. Zubaidi SN, Qadi WSM, Maarof S, Misnan NM, Noor HSM, Hamezah HS, et al. Assessing the Acute Toxicological Effects of *Annona muricata* Leaf Ethanol Extract on Rats: Biochemical, Histopathological, and Metabolomics Analyses. *Toxics.* 2023;11(8):688. DOI: [10.3390/toxics11080688](https://doi.org/10.3390/toxics11080688); PMCID: [PMC10458951](https://pubmed.ncbi.nlm.nih.gov/pmc/PMC10458951/); PMID: [37624193](https://pubmed.ncbi.nlm.nih.gov/37624193/)
25. Ou Z, Zhao J, Zhu L, Huang L, Ma Y, Ma C, et al. Anti-inflammatory effect and potential mechanism of betulinic acid on  $\lambda$ -carrageenan-induced paw edema in mice. *Biomed Pharmacother.* 2019;118:109347. DOI: [10.1016/j.biopha.2019.109347](https://doi.org/10.1016/j.biopha.2019.109347); PMID: [31545273](https://pubmed.ncbi.nlm.nih.gov/31545273/)
26. Makni S, Tounsi S, Rezgui F, Trigui M, Bouassida KZ. *Emex spinosa* (L.) Campd. ethyl acetate fractions effects on inflammation and oxidative stress markers in carrageenan induced paw oedema in mice. *J Ethnopharmacol.* 2019;234:216–24. DOI: [10.1016/j.jep.2018.12.015](https://doi.org/10.1016/j.jep.2018.12.015); PMID: [30552992](https://pubmed.ncbi.nlm.nih.gov/30552992/)
27. Haroon HB, Perumalsamy V, Nair G, Anand DK, Kolli R, Monichen J, et al. Repression of polyol pathway activity by *Hemidesmus indicus* var. *pubescens* R.Br. Linn root extract, an aldose reductase inhibitor: An in silico and ex vivo study. *Nat Prod Bioprospect.* 2021;11(3):315–24. DOI: [10.1007/s13659-020-00290-w](https://doi.org/10.1007/s13659-020-00290-w); PMCID: [PMC8141070](https://pubmed.ncbi.nlm.nih.gov/pmc/PMC8141070/); PMID: [33284412](https://pubmed.ncbi.nlm.nih.gov/33284412/)
28. Li F, Wang Y, Li D, Chen Y, Dou QP. Are we seeing a resurgence in the use of natural products for new drug discovery? *Expert Opin Drug Discov.* 2019;14(5):417–20. DOI: [10.1080/17460441.2019.1582639](https://doi.org/10.1080/17460441.2019.1582639); PMID: [30810395](https://pubmed.ncbi.nlm.nih.gov/30810395/)
29. Sen S, Chakraborty R. Revival, modernization and integration of Indian traditional herbal medicine in clinical practice: Importance, challenges and future. *J Tradit Complement Med.* 2017;7(2):234–44. DOI: [10.1016/j.jtcm.2016.05.006](https://doi.org/10.1016/j.jtcm.2016.05.006); PMCID: [PMC5388083](https://pubmed.ncbi.nlm.nih.gov/pmc/PMC5388083/); PMID: [28417092](https://pubmed.ncbi.nlm.nih.gov/28417092/)
30. Majid N, Nissar S, Raja WY, Nawchoo IA, Bhat ZA. Pharmacognostic standardization of *Aralia cachemirica*: a comparative study. *Futur J Pharm Sci.* 2021;7:33. DOI: [10.1186/s43094-021-00181-y](https://doi.org/10.1186/s43094-021-00181-y)
31. Kao D, Henkin JM, Soejarto DD, Kinghorn AD, Oberlies NH. Non-destructive chemical analysis of a *Garcinia mangostana* L. (Mangosteen) herbarium voucher specimen. *Phytochem Lett.* 2018;28:124–9. DOI: [10.1016/j.phytol.2018.10.001](https://doi.org/10.1016/j.phytol.2018.10.001); PMCID: [PMC6317376](https://pubmed.ncbi.nlm.nih.gov/pmc/PMC6317376/); PMID: [30613309](https://pubmed.ncbi.nlm.nih.gov/30613309/)
32. Noviana E, Indrayanto G, Rohman A. Advances in Fingerprint Analysis for Standardization and Quality Control of Herbal Medicines. *Front Pharmacol.* 2022;13:853023. DOI: [10.3389/fphar.2022.853023](https://doi.org/10.3389/fphar.2022.853023); PMCID: [PMC9201489](https://pubmed.ncbi.nlm.nih.gov/pmc/PMC9201489/); PMID: [35721184](https://pubmed.ncbi.nlm.nih.gov/35721184/)
33. Mboni HM, Faes M, Fraselle S, Compaoré M, Salvius BA, Joseph KB, et al. Evaluating phytochemical constituents and in-vitro antiplasmodial and antioxidant activities of *Fadogiella stigmatoloba*, *Hygrophylla auriculata*, *Hylodesmum*



- repandum, and Porphyrostemma chevalieri extracts. Heliyon. 2023;9(9):e20103. DOI: [10.1016/j.heliyon.2023.e20103](https://doi.org/10.1016/j.heliyon.2023.e20103); PMCID: [PMC10559859](https://pubmed.ncbi.nlm.nih.gov/37809863/); PMID: [37809863](https://pubmed.ncbi.nlm.nih.gov/37809863/)
34. Kong Y, Liu D, Guo X, Chen X. Fluorescence detection of three types of pollutants based on fluorescence resonance energy transfer and its comparison with colorimetric detection. RSC Adv. 2023;13(32):22043-53. DOI: [10.1039/d3ra02647g](https://doi.org/10.1039/d3ra02647g); PMCID: [PMC10359850](https://pubmed.ncbi.nlm.nih.gov/37483672/); PMID: [37483672](https://pubmed.ncbi.nlm.nih.gov/37483672/)
35. Campanale C, Savino I, Massarelli C, Uricchio VF. Fourier Transform Infrared Spectroscopy to Assess the Degree of Alteration of Artificially Aged and Environmentally Weathered Microplastics. Polymers. 2023;15(4):911. DOI: [10.3390/polym15040911](https://doi.org/10.3390/polym15040911); PMCID: [PMC9961336](https://pubmed.ncbi.nlm.nih.gov/36850194/); PMID: [36850194](https://pubmed.ncbi.nlm.nih.gov/36850194/)
36. Pakkirisamy M, Kalakandan SK, Ravichandran K. Phytochemical Screening, GC-MS, FT-IR Analysis of Methanolic Extract of Curcuma caesia Roxb (Black Turmeric). Pharmacogn J. 2017;9(6):952-6. DOI: [10.5530/pj.2017.6.149](https://doi.org/10.5530/pj.2017.6.149)
37. Erhirhie EO, Ihekwereme CP, Ilodigwe EE. Advances in acute toxicity testing: strengths, weaknesses and regulatory acceptance. Interdiscip Toxicol. 2018;11(1):5-12. DOI: [10.2478/intox-2018-0001](https://doi.org/10.2478/intox-2018-0001); PMCID: [PMC6117820](https://pubmed.ncbi.nlm.nih.gov/30181707/); PMID: [30181707](https://pubmed.ncbi.nlm.nih.gov/30181707/)
38. Abdel-Moneim AM, Al-Kahtani MA, El-Kersh MA, Al-Omar MA. Free Radical-Scavenging, Anti-Inflammatory/ Anti-Fibrotic and Hepatoprotective Actions of Taurine and Silymarin against CCl4 Induced Rat Liver Damage. PLoS One. 2015;10(12):e0144509. DOI: [10.1371/journal.pone.0144509](https://doi.org/10.1371/journal.pone.0144509); PMCID: [PMC4676695](https://pubmed.ncbi.nlm.nih.gov/26659465/); PMID: [26659465](https://pubmed.ncbi.nlm.nih.gov/26659465/)
39. Boussouf L, Boutennoune H, Kebieche M, Adjeroud N, Al-Qaoud K, Madani K. Anti-inflammatory, analgesic and antioxidant effects of phenolic compound from Algerian Mentha rotundifolia L. leaves on experimental animals. S Afr J Bot. 2017;113:77-83. DOI: [10.1016/j.sajb.2017.07.003](https://doi.org/10.1016/j.sajb.2017.07.003)
40. Senthamilselvi MM, Kesavan D, Sulochana N. An anti-inflammatory and anti-microbial flavone glycoside from flowers of Cleome viscosa. Org Med Chem Lett. 2012;2(1):19. DOI: [10.1186/2191-2858-2-19](https://doi.org/10.1186/2191-2858-2-19); PMCID: [PMC3493290](https://pubmed.ncbi.nlm.nih.gov/22613049/); PMID: [22613049](https://pubmed.ncbi.nlm.nih.gov/22613049/)
41. Salem S, Leghouchi E, Soulimani R, Bouayed J. Reduction of paw edema and liver oxidative stress in carrageenan-induced acute inflammation by Lobaria pulmonaria and Parmelia caperata, lichen species, in mice. Int J Vitam Nutr Res. 2021;91(1-2):143-51. DOI: [10.1024/0300-9831/a000620](https://doi.org/10.1024/0300-9831/a000620); PMID: [31847731](https://pubmed.ncbi.nlm.nih.gov/31847731/)
42. Mansouri MT, Hemmati AA, Naghizadeh B, Mard SA, Rezaie A, Ghorbanzadeh B. A study of the mechanisms underlying the anti-inflammatory effect of ellagic acid in carrageenan-induced paw edema in rats. Indian J Pharmacol. 2015;47(3):292-8. DOI: [10.4103/0253-7613.157127](https://doi.org/10.4103/0253-7613.157127); PMCID: [PMC4450555](https://pubmed.ncbi.nlm.nih.gov/26069367/); PMID: [26069367](https://pubmed.ncbi.nlm.nih.gov/26069367/)